SUPPLEMENTARY DATA

In this study, we investigate the impact of type 1 diabetes on brain growth in young children, including glycemic effects, and correlations between cognitive performance and key brain variables. Expanded details of methodology and results are included in this Appendix. All tables and Figures labeled numerically with an "A".

METHODS

Supplementary Figure 1 A. Protocol flow chart (numbers in parenthesis are those that used CGM at least 3d each visit)

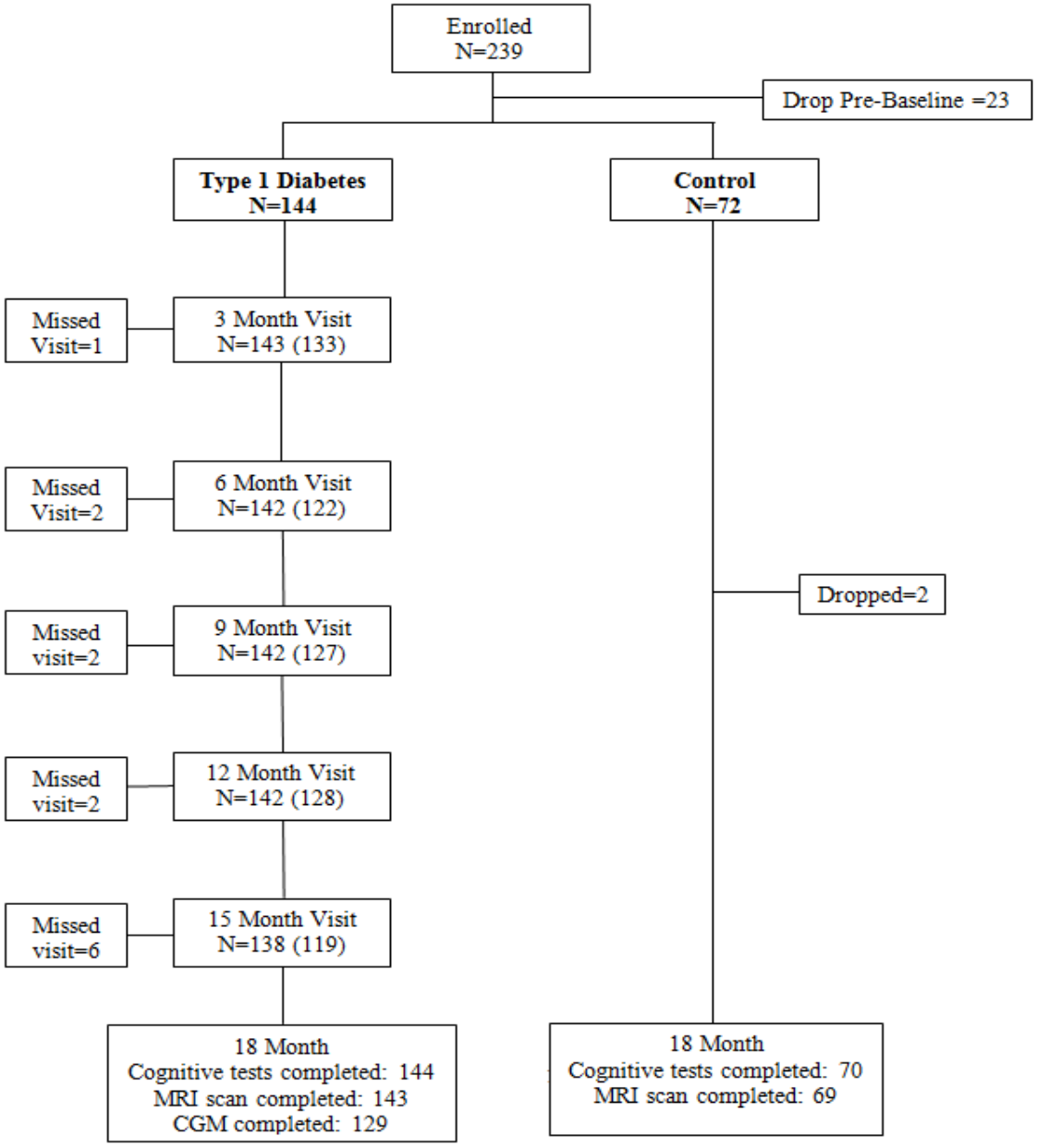

SUPPLEMENTARY DATA

Supplementary Table 1A. Neurocognitive Test Battery: Domains and Measures

Cognitive Domain	**Measure** *	**Test**	**Battery** †
Intelligence Quotient	scaled score ‖	Block design	WPPSI3 / WASI
	scaled score ‖	Similarities	
	scaled score ‖	Vocabulary	
	scaled score ‖	Matrix reasoning	
Executive Functions	Detectability	CPT2	Connor's
	Total Correct	Auditory Attn	NEPSYII
	Total Correct	Concept Formation	WJIII Cognitive
	Total Correct	Numbers	CMS
Learning & Memory	Total items recalled	Word Lists ‡	CMS
	Total items recalled	Dot Locations ‡	CMS
Processing Speed	standard score §	Visual Match I / II	WJIII Cognitive
		Decision Speed	WJIII Cognitive
Mood/Behavior	**Measure**	**Scale**	**Battery**
Executive functioning	Raw score	Global Executive Composite	BRIEF Parent
Externalizing symptoms	T score	Externalizing	BASCII PRS
Internalizing symptoms	T score	Internalizing	BASCII PRS
Covariate	**Measure**	**Test**	**Battery**
Parent Intelligence Quotient	scaled score ‖	Vocabulary	WASI
	scaled score ‖	Matrix Reasoning	

* – *z* score was calculated for each measure using mean and SD from the current study pooling all participants. For domains with more than one test, the average was taken giving equal weight to each *z* score.

† – Abbreviations: CMS – Children's Memory Scale(1); CPT – Continuous Performance Test(2); NEPSYII – Neuropsychological Battery for Children, Second Edition(3); WJIII Cognitive – Woodcock-Johnson Test of Cognitive Abilities, Third Edition (4); WPPSI3–Wechsler Preschool and Primary Scales of Intelligence, Third Edition(5); WASI-Wechsler Adult Scale of Intelligence; BRIEF – Behavior Rating Inventory of Executive Functions(6); BASCII PRS – Behavior Assessment System for Children, Second Edition Parent Rating Scales(7).

‡ – Same version given regardless of age.

§ – Age-based standard score from WJIII Cognitive normative update (NU) sample

‖– Age-based scaled score derived from Wechsler normative sample

Scores were omitted in participants missing sub-domain measures.

SUPPLEMENTARY DATA

Imaging

Screening of scans: 216 participants were entered into the study, 211 had image data at both baseline and 18-months time points, and 201 subjects (135 T1D, 66 controls) were used for the longitudinal VBM analysis. Scans from participants were excluded if they did not pass a visual quality review of brain tissue segmentation at one of the time points (N=5 participants), or if they did not have consistent segmentations across time points (N=5 other participants). The latter criterion was utilized to exclude those with unusually large (>2.5 SD) differences in total gray or white matter volume across time points relative to differences for the entire group. The ten excluded participants included 7 children with diabetes and 3 controls. Glycemic values of the excluded T1D subjects were not different relative to the overall diabetes group, suggesting the outliers were due to image processing artifacts.

Imaging Data Acquisition:

All six imaging sites utilized a Siemens 3T Tim Trio whole body MR system and a standard 12-channel head coil using identical imaging protocols uploaded to every scanner. Sagittal T1 images of the brain were acquired (right to left) using a magnetization prepared rapid gradient echo (MP-RAGE) pulse sequence with the following parameters: repetition time [TR] = 2300 ms, echo time [TE] = 2.98 ms, inversion time [TI] = 900 ms, flip angle=9°, slice thickness = 1 mm, FOV = 25.6 cm x 24 cm, 160 slices, matrix = 256x256, voxel size =1.0x1.0x1.0 mm, and duration = 4:54 minutes. By default, two MP-RAGE acquisitions were obtained for all participants to increase the probability that at least one scan would be collected with minimal head motion (8). A second MRI was performed on a separate day if the initial scan could not be completed or if image quality was deemed unacceptable after the first attempt.

Structural Analyses: We measured growth rates of total and regional gray and white matter volumes.

Total gray and white matter volumes. Images were segmented into gray and white matter using well-established voxel-based morphometry methods in Statistical Parametric Mapping software (SPM8, Wellcome Department of Imaging Neuroscience, University College London, http://www.fil.ion.ucl.ac.uk/spm) in MATLAB (The MathWorks, Natick, MA). Data were corrected for magnetic field inhomogeneity and subsequently segmented into gray matter and white matter, and cerebrospinal fluid volumes based on a priori tissue probability maps and spatially constrained tissue classification based on neighboring voxels (9; 10). Total gray and white matter volumes were calculated in native space before any morphological deformations. Total gray matter volume included cortical, subcortical, and cerebellar gray matter, while total white matter volume included cerebral and cerebellar white matter, as well as thalamus, midbrain, pons, and medulla.

Regional brain volumes. Starting with the segmented images, images for each participant were rotated into a common space, and high dimensional inter-subject registration was then performed using the DARTEL toolbox in SPM (11). Images were warped and modulated into Montreal Neurological Institute (MNI) space for reporting of results, down-sampled to 1.5×1.5×1.5mm voxels, and spatially smoothed using a 6 mm full-width at half-maximum (FWHM) Gaussian smoothing kernel. White matter regions with significant differences were classified with a white matter atlas (12), but the tract identifications are approximate because directional information of white matter tracts is not available in a voxel-based morphology study.

SUPPLEMENTARY DATA

Statistics

Prospective growth of total gray and white matter volume for the between-group analysis was analyzed in SPSS using repeated measures while controlling for age at baseline, sex, and interval between two time points. Correlations of structural changes with glycemic variables were investigated by including the glycemic variables in the same repeated-measures model. Correlations with the difference of glycated hemoglobin values at baseline and 18-months used the difference of the glycated hemoglobin values as the covariate of interest.

For voxel based morphology analyses, growth was measured as the difference of the images from time 1 to time 2 (13; 14). All analyses applied a voxel wise height threshold of $p<0.05$, corrected for non-stationary smoothness of the data, covaried for age, sex, total gray (or white) matter volume, and interval between the two time points. We report regional significant results at $p<0.05$ corrected for Family-Wise Error. Average correlations of the cluster were calculated by using the cluster as a region-of-interest (ROI), extracting the mean over the ROI for each subject, and correlating with the glycemic variable while controlling for all other parameters. For large clusters, we localized the subregions with the strongest statistical effects by raising the voxelwise threshold to $p<0.01$, and reporting significant clusters after correction for Family-Wise Error. Correlations with SD and MAGE were covaried by gluMean to help discriminate between the effects of glucose variability and glucose mean. Correlations with diffAUC6% were covaried by avgHbA1c to discriminate between the effects of very high glucose and mean glucose levels.

Correlations

We analyzed the correlation between differences in IQ across time points with differences in total GMV (WMV). Using SPSS, repeated measures of overall IQ were correlated with the change in GMV (WMV), while controlling for GMV at time 1, age at time1, sex, and the interval between the two time points. Significant results are reported for $p<.05$.

Multisite Effects

Identical scanners were used at each site and calibrations were performed on an ongoing basis to confirm the repeatability of measurements across sites. Two adult human phantoms were scanned on every machine prior to the start of the study and again annually for two years. A standard plastic phantom (American College of Radiology [ACR]) was also scanned quarterly at each site to monitor for possible temporal variations in scan quality. Additional human and/or ACR data were acquired both before and after hardware or software upgrades. We observed less than 0.5% variation in geometric size across sites, which was not significantly larger than the observed intrasite variation of 0.4%. These results suggested robust and stable MRI imaging, and were well within the variation ranges reported for other large multisite studies using identical scanners (14-16). A factorial design (17) used to investigate scanner effects on the voxel based morphology results showed one small region that was significant for the main effect of scanner. Potentially significant results in this region were reanalyzed after including the effect of scanner as described (18).

SUPPLEMENTARY DATA

RESULTS

Supplementary Table 2A. Mean (± SD) total brain volumes in cubic centimeters (cc)

GROUP	N	Age (yrs) Time 1	Gray Matter Time 1	Gray Matter Time 2	White Matter Time 1	White Matter Time 2
Diabetes	135	7.05 (1.7)	689 (53)	699 (52)	446 (40)	457 (40)
males	72	6.96 (1.8)	712 (52)	722 (51)	464 (40)	476 (40)
females	63	7.14 (1.5)	664 (40)	672 (39)	426 (28)	437 (28)
Control	66	7.00 (1.8)	690 (48)	704 (47)	447 (38)	460 (38)
males	35	7.34 (1.9)	711 (49)	725 (48)	465 (35)	478 (33)
females	31	6.61 (1.5)	666 (43)	680 (43)	427 (32)	440 (33)

Time 1 - baseline, Time 2 – 18-months

SUPPLEMENTARY DATA

REFERENCES for APPENDIX

1. Cohen MJ: CMS: Children's Memory Scale The Psychological Corporation, 1997
2. Connors CK: CPT: The Conners Continuous Performance Test. Toronto, Canada, Multi-Health Systems, 1994
3. Korkman M, Kirk U, Kemp S: NEPSY-II: Neuropsychological Battery for Children, Second Edition. San Antonio, TX, Harcourt Assessment 2007
4. Woodcock RW, McGrew KS, Mather N: Woodcock-Johnson Test of Cognitive Abilites, Third Edition. Itasca, IL, Riverside Publishing 2001
5. Wechsler D: Wechsler Preschool and Primary Scale of Intelligence, Third Edition. San Antonio, TX, Psychological Corporation, 2002
6. Gioia GA, Isquith PK, Guy SC, Kenworthy L: Behavior Rating Inventory of Executive Function. Lutz, FL, PAR, Inc., 2000
7. Reynolds CR, Kamphaus RW: Behavior Assessment System for Children, Second Edition Parent Rating Scales. Circle Pines, MN, American Guidance Service, 2004
8. Jack CR, Jr., Bernstein MA, Fox NC, Thompson P, Alexander G, Harvey D, Borowski B, Britson PJ, J LW, Ward C, Dale AM, Felmlee JP, Gunter JL, Hill DL, Killiany R, Schuff N, Fox-Bosetti S, Lin C, Studholme C, DeCarli CS, Krueger G, Ward HA, Metzger GJ, Scott KT, Mallozzi R, Blezek D, Levy J, Debbins JP, Fleisher AS, Albert M, Green R, Bartzokis G, Glover G, Mugler J, Weiner MW: The Alzheimer's Disease Neuroimaging Initiative (ADNI): MRI methods. *J Magn Reson Imaging* 27:685-691, 2008
9. Ashburner J, Friston KJ: Unified segmentation. *NeuroImage* 26:839-851, 2005
10. Zhang Y, Brady M, Smith S: Segmentation of brain MR images through a hidden Markov random field model and the expectation-maximization algorithm. *IEEE Trans Med Imaging* 20:45-57, 2001
11. Ashburner J: A fast diffeomorphic image registration algorithm. *NeuroImage* 38:95-113, 2007
12. Oishi K, Faria A, Van Zijl P, Mori S: *MRI atlas of human white matter*, Academic Press, 2011
13. Chételat G, Landeau B, Eustache F, Mézenge F, Viader F, de la Sayette V, Desgranges B, Baron JC: Using voxel-based morphometry to map the structural changes associated with rapid conversion in MCI: A longitudinal MRI study. *NeuroImage* 27:934-946, 2005
14. Takao H, Hayashi N, Ohtomo K: Effect of Scanner in Longitudinal Studies of Brain Volume Changes. *J Magn Reson Imaging* 34:438-444, 2011
15. Han X, Jovicich J, Salat D, van der Kouwe A, Quinn B, Czanner S, Busa E, Pacheco J, Albert M, Killiany R, Maguire P, Rosas D, Makris N, Dale A, Dickerson B, Fischl B: Reliability of MRI-derived measurements of human cerebral cortical thickness: The effects of field strength, scanner upgrade and manufacturer. *Neuroimage* 32:180-194, 2006
16. Jovicich J, Czanner S, Han X, Salat D, van der Kouwe A, Quinn B, Pacheco J, Albert M, Killiany R, Blacker D, Maguire P, Rosas D, Makris N, Gollub R, Dale A, Dickerson BC, Fischl B: MRI-derived measurements of human subcortical, ventricular and intracranial brain volumes: Reliability effects of scan sessions, acquisition sequences, data analyses, scanner upgrade, scanner vendors and field strengths. *Neuroimage* 46:177-192, 2009
17. Stonnington CM, Tan G, Klöppel S, Chu C, Draganski B, Jack Jr CR, Chen K, Ashburner J, Frackowiak RSJ: Interpreting scan data acquired from multiple scanners: A study with Alzheimer's disease. *Neuroimage* 39:1180-1185, 2008
18. Marzelli MJ, Mazaika PK, Barnea-Goraly N, Hershey T, Tsalikian E, Tamborlane W, Mauras N, White NH, Buckingham B, Beck RW, Ruedy KJ, Kollman C, Cheng P, Reiss AL, for the Diabetes Research in Children N: Neuroanatomical Correlates of Dysglycemia in Young Children With Type 1 Diabetes. *Diabetes* 63:343-353, 2014